Supporting Information

Quartz nanopillar hemocytometer for high-yield separation and counting of $CD4^+$ T lymphocytes

Dong-Joo Kim[1], Jin-Kyung Seol[1], Yu Wu[2], Seungmuk Ji[3], Gil-Sung Kim[1], Jung-Hwan Hyung[1], Seung-Yong Lee[1], Hyuneui Lim[3], Rong Fan[†2,4], and Sang-Kwon Lee[††1,2]

[1]Department of Semiconductor Science and Technology, Chonbuk National University, Jeonju 561-756, Korea

[2]Department of Biomedical Engineering, Yale University, New Haven, CT 06511, USA

[3]Department of Nature-Inspired Nanoconvergence Systems, Korean Institute of Machinery and Materials (KIMM), Daejeon 305-343, Korea

[4]Yale Comprehensive Cancer Center, New Haven, CT 06520, USA

Corresponding authors:

[†]E-mail: rong.fan@yale.edu, tel: 1-203-432-9905

[††] E-mail: sk_lee@chonbuk.ac.kr and sangkwon.lee@yale.edu, tel: +82-63-270-3973

1. Effect of O_2 plasma treatment on QNP surface

Figure S1 shows a flow cytometric analysis of surface-bound $CD4^+$ T-lymphocytes on the STR-QNP arrays after O_2 plasma treatment on the surface prior to STR immobilization. After O_2 plasma treatment, the percentage of $CD4^+$ T lymphocytes in cell suspensions dramatically decreased from ~33.9% to ~1.5% (corresponding to ~95.3 ± 1.1% in a cell separation yield of $CD4^+$ T lymphocytes, right panel). The percentage of $CD4^+$ T lymphocytes was determined to be about 7.6 % (corresponding ~78.5 ± 6.1% in the cell separation yield, right panel), roughly five times higher than that of O_2-treated STR-QNR arrays. The capture yield of $CD4^+$ T lymphocytes with and without O_2 treatment in the QNP arrays is summarized in Figure S1 (bar graph and table in right panel). These results correspond well with our previous reports on STR-functionalized silicon nanowire (SiNW) arrays on Si wafers. We also confirmed that hydroxyl group conferment on QNP arrays through O_2 plasma treatment is one of the crucial steps for the STR immobilization and further improvement of $CD4^+$ T lymphocyte capture efficiency, since hydroxyl groups allow the QNP arrays to improve conjugation with APTES.

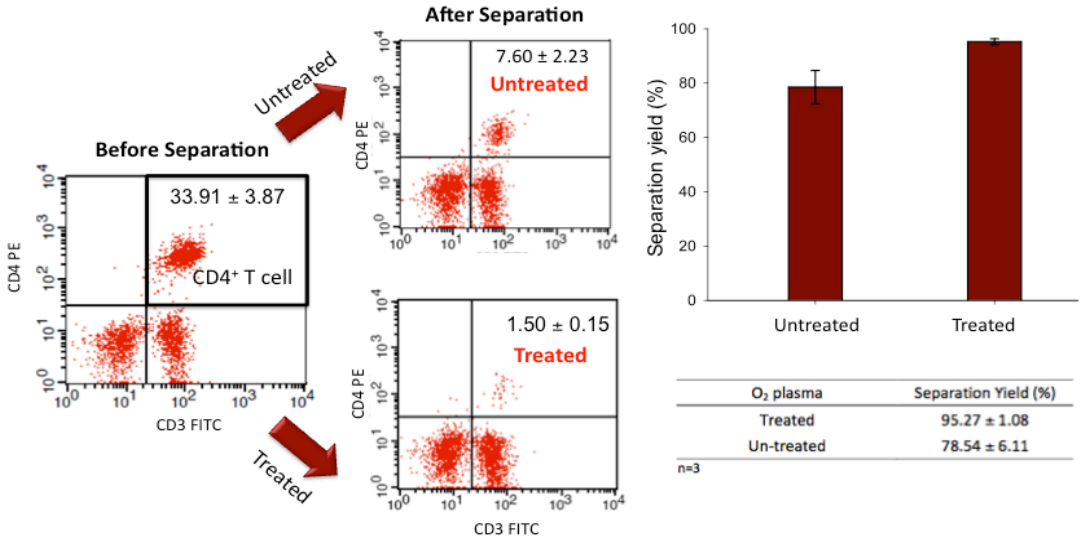

Figure S1. Flow cytometric analysis of the $CD4^+$ T lymphocytes after binding O_2 plasma-treated and –untreated STR-QNP arrays (left panel). The averaged cell separation efficiency is summarized with bar graphs (top right panel) and the table (bottom right panel).

2. Recycling effect of STR-functionalized QNP arrays

To investigate the possibility of the recycling of the STR-QNP arrays, the arrays were washed out using standard organic cleaning process after one to three uses. The cleaning process was performed using a mixture of sulfuric acid (H_2SO_4) and hydrogen peroxide (H_2O_2) for 10 to 20 min, known as piranha cleaning (96% H_2SO_4 : 30% H_2O_2 = 1 : 1). This mixture was also used to remove organic residues from the surface. Subsequently, the QNP array surface was rinsed with deionized (DI) water. The cleaning process was finished by air blowing to dry the QNP arrays. Figure S2 shows the capture efficiency of the recycled STR-QNP arrays after three uses, indicating that there was no significant change in the capture efficiency (92.5 ± 4.2% for sample 1 and ~ 91.5 ± 3.5% for sample 2, bottom table in Figure S2) of $CD4^+$ T lymphocytes after three cycles. Our results suggest that the piranha cleaning process helped to remove all organic and chemical substances on the QNP substrate, and allowed the STR-QNP arrays to be able to be used repeatedly without severe surface degradation.

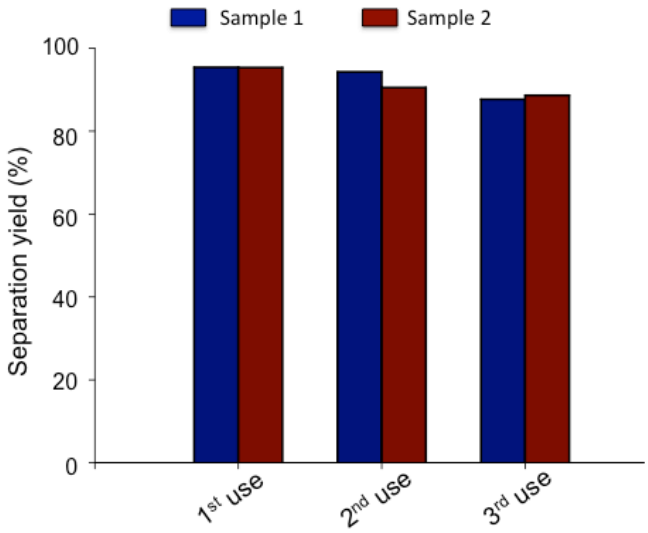

Re-used sample	Separation Yield (%)
Sample 1	92.47 ± 4.18
Sample 2	91.51 ± 3.45

* Each sample was reused three times after piranha cleaning

Figure S2. Cell separation efficiency (yield) of STR-QNP arrays after three uses, indicating no significant degradation in cell separation efficiency after recycled.

3. Large-scale cell visualization and enumerating of captured cells using STR-QNP arrays

Figure S3a shows a photograph of the STR-functionalized QNP arrays with PDMS top layer involving nine wells (5 mm in diameter). To identify the captured T-lymphoblasts, the cells were stained using FITC-CD3-Ab and APC-CD4-Ab. Figures S3b-c show optical (×100) images together with immunofluorescence-stained images of separated T-lymphoblasts on the STR-QNP arrays, thereby indicating that all T-lymphoblasts were well distributed on the surface.

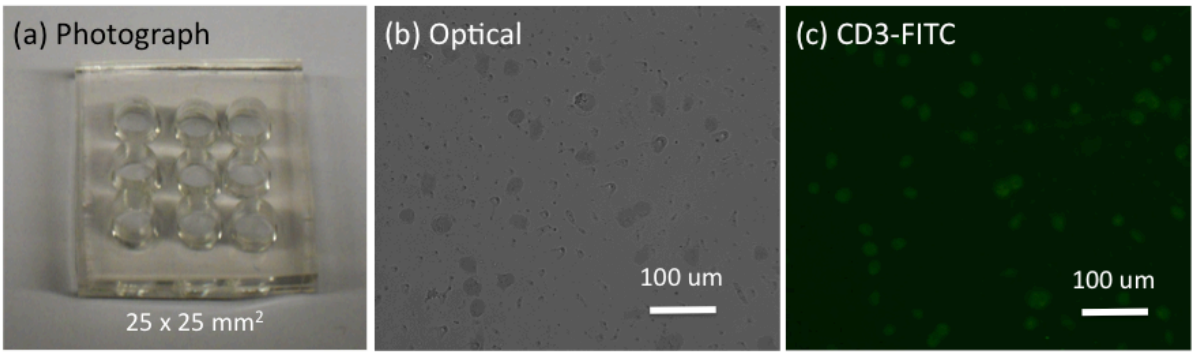

Figure S3. (a) Photograph of the STR-functionalized QNP arrays with PDMS top layer involving nine wells (5 mm in diameter). (b)-(c) Optical and florescence images of captured T-lymphoblasts cells on STR-QNP arrays.

The fluorescence image shown in Figure S3c shows that most immobilized on the STR-QNP arrays expressed both CD4 and CD3 with good agreement with respect to the T-lymphoblast (CCRF-CEM) flow cytometric analysis. Figures S4a-c show microarray-scanned images of immobilized the $CD4^+$ T-lymphoblasts (CCRF-CEM) on the STR-functionalized eight QNP wells with enlarged images. As shown in Figure S4, the cell population of surface-bound CD4+ T-lymphoblasts on the large-scale STR-QNP arrays increased with an increasing number of loaded cells into the wells. This also indicates that the loaded cells are evenly allocated on the QNP arrays.

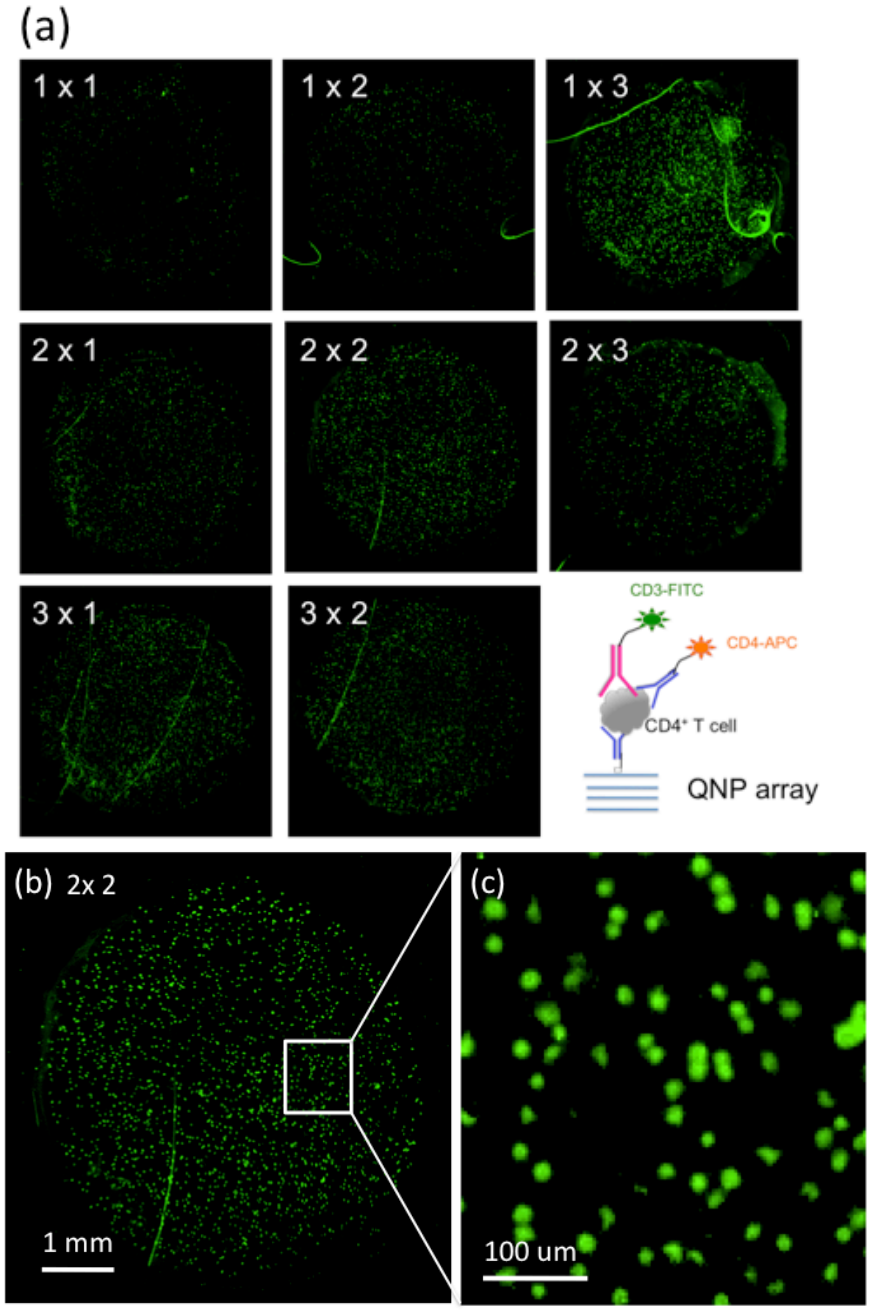

Figure S4. (a) Immunofluorescence-stained T-lymphoblasts (human breast cancer cell line, CCRF-CEM cell line) on large-scale STR-functionalized QNP arrays for each well (total of eight wells). (b)-(c) Higher magnification images of immunofluorescent staining of the captured T-lymphoblasts in 2×2 well, introducing 2,500 cells, on the QNP arrays.